

# Industrial Applications of Online Monitoring of Drying Processes of Drug Substances Using NIR

Jens Burgbacher and Jacques Wiss\*

Novartis Pharma AG, Basel, Switzerland

## Abstract:

Drying is an important part of manufacturing processes in the chemical and pharmaceutical industry. The product quality often depends on the drying conditions and efficiency. Moreover, this unit operation frequently represents the bottleneck of the whole process. Therefore, online monitoring of the drying operation can lead to a significant improvement of the cycle time as well as to a reduction of the analytical work and costs. This paper demonstrates the effectiveness of NIR spectroscopy to control drying processes on an industrial scale. The examples shown in this study are realized using different kinds of dryers (filter dryer, paddle dryer, and spherical dryer) and various solvents (water and organic solvents). The spectral data are evaluated using multivariate calibration methods (partial least squares regression). These studies show that the solvent concentrations determined using NIR are in good agreement with the reference analyses. Moreover, the direct measurement in the powder allows stopping the drying process at a given residual solvent concentration (which is crucial in certain processes, e.g. to obtain specific hydrate forms). All together, the implementation of NIR for online monitoring of drying processes leads to a significant optimization of plant equipment utilization and to a higher throughput while reducing the risk of out-of-specifications batches.

## Introduction

Drying is an essential part of the manufacturing process of APIs. With a crystalline product, it is necessary to ensure that the crystals are not damaged or modified during drying, and in the case of pharmaceutical products care must be taken to avoid contamination.

Several potential problems can occur during the drying of active pharmaceutical ingredients (APIs): (a) quality variability (e.g., due to overdrying and formation of undesired decomposition products), (b) too long duration of cycle time (drying is often the bottleneck of processes due to the long time needed for this unit operation) (c) poor optimization of equipment use (this is a consequence of the long cycle time: the improvement of the plant productivity avoids buying additional dryers and leads to a significant costs reduction).

The current methods for determining the end point of drying processes require either stopping at the preset ending time for the process and waiting for residual solvent data to be collected or proceeding, at risk, to the next unit operation. The ability to online monitor drying processes will minimize the need for off-line residual solvent analysis and allow improved control of

the process and reduced cycle time. Further, the method allows for better use of manufacturing capability by minimizing the time a product spends in the dryer, which also minimizes the stress to the material from overdrying (i.e., product degradation, crystal form changes) and reduces safety concerns involving operator exposure.

The aim of this paper is to present some applications of NIR spectroscopy for the online monitoring of drying processes in the industrial scale.

**Classical Determination of the Drying End Point.** The residual solvent content of a material is usually expressed as a percentage of the weight of the dry material. The residual solvent may be present in the following two forms.<sup>1</sup>

*Bound Residual Solvent.* This is solvent retained in such a way that it exerts a vapour pressure less than that of the free solvent at the same temperature. Such solvent may be retained in small capillaries or adsorbed on surfaces.

*Free Residual Solvent.* This is solvent which is in excess of the equilibrium moisture content.

In the drying of materials, it is necessary to remove free residual solvent from the surface and also from the interior.

Several off-line residual solvent content measurements are usually used in the pharmaceutical and chemical industry.

- The residual solvent content of samples collected during the drying process can be determined by loss of drying (LOD). Accurately weighed samples are placed in wide-mouth glass jars. After drying in a convection oven until a constant weight is obtained, the samples are weighed again, and the mass loss is recorded as the residual solvent content on a percent weight/weight basis.

- For powders containing water, the Karl Fischer coulometric or volumetric titration is a common method. The Karl Fischer titration method has advantages over simple “loss on drying” methods of moisture determination because it is specific to water. Loss on drying will detect the loss of *any* volatile substance.

- GC head space: the sample is transferred in a vial sealed against gas and heated up to a defined temperature. The headspace is analyzed with GC when the equilibrium between the sample and the vapor phase is reached.

Some of these off-line measurements require breaking vacuum at individual time points and sampling of the wet cake.

Several previous studies concerning applications of online monitoring of drying processes, mainly in laboratory or pilot-plant scale are described in the literature. Various measurement strategies and techniques were used:

\* Correspondence author: Novartis Pharma AG, Building WSJ-145.11.54, CH-4002 Basel, Switzerland. E-mail: jacques.wiss@novartis.com.

### Monitoring of the Vapor Stream in the Vacuum Line.

This can be done using either mass spectrometry<sup>2</sup> or spectroscopy.<sup>3</sup> In the case of mass spectrometry (MS), the ions are separated according to their mass-to-charge ratio and detected after ionization of the sample. The signal is then sent to the data system with the relative abundance of these ions. The advantage of this technique is that little or no method development is required other than to select the ions of interest. The masses of interest can be determined from a simple scan of the solvents to determine the mass fragment pattern or by simply referring to a mass spectral library available on many MS software packages. In the case of spectroscopy (e.g., NIR or Mid-IR), a gas cell should be used. This probe should be thermostatted to avoid spectral variations due to the temperature changes. An advantage of this kind of monitoring is that the sampling from the vacuum line of the dryer is inherently more homogeneous compared with a direct measurement in the powder. These methods can lead to an effective determination of the drying end point if a complete drying of the powder is desired or if the solvent is not bound in the crystals. In all other cases, a direct measurement in the powder is preferable.

**Monitoring of the Current Solvent Concentration Directly in the Powder.** Most of the previous papers present the implementation of NIR in fluidized bed granulators.<sup>4-7</sup> The main disadvantage of spectroscopy is that this method requires a cleaning of the probe before each run. Moreover, a chemometric model must be established for quantitative predictions of the solvent concentration. For powders containing water, the end-point determination of drying can also be performed using microwave resonance technology.<sup>8</sup> Water molecules are strong dipoles. When an electromagnetic field is produced, the water molecules adjust themselves according to the field's polarity, due to their positive and negative ends. If the field changes its polarity rapidly, only the water molecules can follow this change in direction as they are small and have a strong dipole. This movement requires energy, which is drawn from the electromagnetic field. This loss of energy, which depends on the number of water molecules, is being detected.

In the chemical production, drug substances are often not completely dried and very often contain organic solvents. Therefore, it was decided to monitor the residual solvent concentration directly in the crystals to determine the real residual solvent values. Many dryers are in multipurpose plants, and NIR is the favorite technique due to its polyvalence. This paper presents the results of the implementation of NIR spectrometry in various types of dryers in production plants.

- (1) Coulson, J. M.; Richardson, J. F. *Chemical Engineering, Vol. 2 Unit Operations*; Pergamon Press: Oxford, 1978; pp 710-711..
- (2) Hettenbach, K.; Am Ende, D. J.; Dias, E.; Brenek, S. J.; Laforte, C.; Barnett, S. M. *Org. Process Res. Dev.* **2004**, *8*, 867-872.
- (3) Harris, S. C.; Walker, D. S. *J. Pharm. Sci.* **2000**, *89* (No. 9), 1180-1186.
- (4) Findlay, W. P.; Peck, G. R.; Morris, K. R. *J. Pharm. Sci.* **2005**, *94* (No. 3), 604-612.
- (5) Frake, P.; Greenhalgh, D.; Grierson, S. M.; Hempenstall, J. M.; Rudd, D. R. *Int. J. Pharm.* **1997**, *151*, 75-80.
- (6) Rantanen, J.; Lehtola, S.; Rämät, P.; Mannermaa, J. P.; Yliruusi, J. *Powder Technol.* **1998**, *99*, 163-170.
- (7) Green, R. L.; Thurau, G.; Pixley, N. C.; Mateos, A.; Reed, R. A.; Higgins, J. P. *Anal. Chem.* **2005**, *77*, 4515-4522.
- (8) Buschmüller, C.; Wiedey, W.; Dressler, J.; Döscher, C.; Breitreutz, J. *2nd European Congress on Life Science Process Technology*, Nuremberg, March 2007.

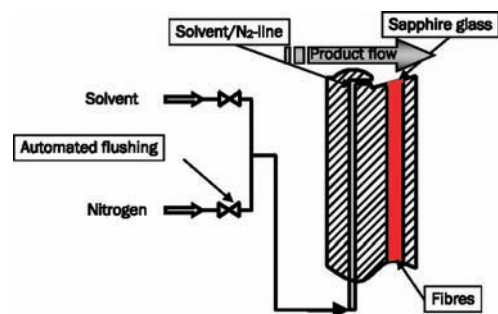


Figure 1. Drawing of the diffuse reflectance NIR probe.

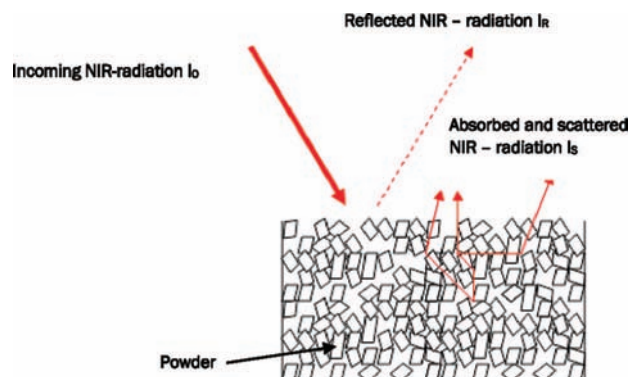


Figure 2. Diffuse reflectance in a powder.

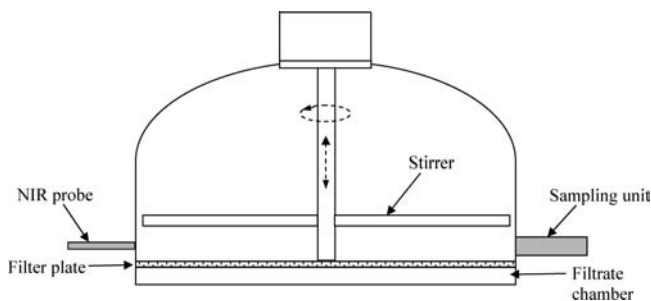
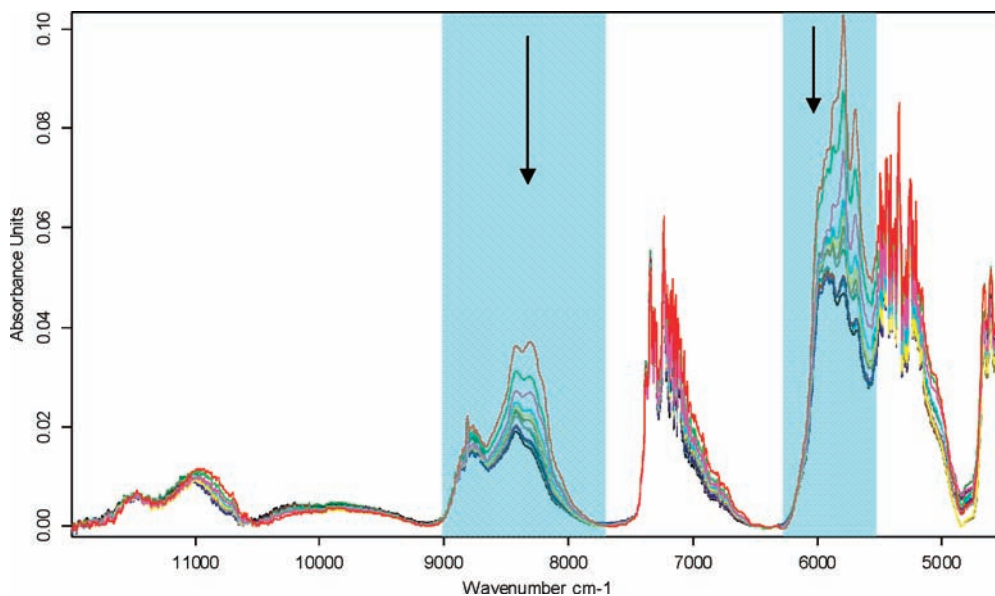


Figure 3. Installation of the NIR probe in the Nutsche filter dryer (powder A).

**Equipment for the Spectroscopic Measurements.** The experiments were performed with a NIR Spectrometer Matrix F (Bruker Optics). This spectrometer was equipped with a Reflector reflection immersion probe (Solvias). The optic material is sapphire (illuminated spot with a diameter of 3 mm), and the body of this probe is made of hastelloy. The probe is connected to the spectrometer with a 30 m fiber-optic cable (each connection cable is made of seven glass fibers). The probe used is equipped with an integrated flushing system, which allows cleaning the sapphire window with either nitrogen or a solvent before a new batch or between two data measurements. The substance flow must be against the incline of the sapphire window to guarantee a direct contact with the powder and to avoid obstructing the hole of the flushing system. Figure 1 shows the schematic construction of the probe and the direction of the powder flow (which is also the rotation direction of the stirrer in the case of a stirred dryer).

The experimental conditions were the following: resolution: 8 cm<sup>-1</sup> and number of scans: 100-300 (duration: ~1-3 min., depending on the powder).



**Figure 4.** Spectra during the drying of powder A in the Nutsche filter dryer (the shaded areas are the ranges used for the calibration).

**Table 1.** Cross validation of the model used for the monitoring of S1 and S2 concentrations (Powder A)

| solvent | frequency range                          | data preprocessing   | number of factors | RMSECV [mass %] | $R^2$ |
|---------|--|--|-------------------|-----------------|-------|
| S1      | 5500–6200 and 7700–9000 $\text{cm}^{-1}$ | first derivative and straight line subtraction               | 3                 | 1.02            | 96.93 |
| S2      | 5500–6200 and 7700–9000 $\text{cm}^{-1}$ | first derivative and MSC (multiplicative scatter correction) | 5                 | 0.24            | 82.31 |

**Diffuse Reflectance.** Figure 2 summarizes the principle of the diffuse reflectance for powders. A part of the light emitted by the spectrometer is absorbed in the powder and scattered in all directions of the space. The weak diffuse radiation is collected in a manner which minimizes the specular reflectance component and is measured by the spectrometer.

A reference spectral intensity is measured prior to the beginning of the system calibration using a Spektral disk (mixture of barium sulfate and Teflon). The pseudoabsorbance during the spectral measurements with powders is calculated according to eq 1.

$$A = -\log\left(\frac{I_{\text{Sample}}}{I_{\text{Reference}}}\right) = \log\left(\frac{1}{R}\right) \quad (1)$$

with  $R$  = reflectance.

**PLS Calibration.** To calibrate the NIR analysis system, many calibration samples are needed. They should contain each component of interest in various concentrations. These concentrations must be determined by a different analytical method and correlated with the corresponding NIR spectra to develop a chemometric model (partial least squares PLS regression method<sup>9</sup>). This model is the calibration function used for the analysis of unknown samples. Before using the model for routine application, its prediction capability must be tested (validation).

**First Example: Nutsche Filter Dryer.** This device is a combination of a filter (Nutsche) and of a dryer. A suspension can be loaded in the apparatus, the mother liquor can be filtered off by overpressure or depression, and the obtained filter cake can be washed and finally thermally dried. The stirrer, the vessel walls, and sometimes the bottom of the device can be heated for the drying operation. An advantage of this kind of dryer is that several process steps can be performed in the same apparatus, thus avoiding the handling of potentially toxic compounds and reducing the loss of very costly substances.

The active substance (powder A) contains two organic solvents (S1 and S2). The criterion for the drying end point is that the sum of both solvents should be below 15 wt %. This is not the final step of the process, and this powder should be worked up before its final drying. Nevertheless, the required criterion is important to guarantee the quality of the final product.

The probe was installed on a 6 m<sup>2</sup> Nutsche filter dryer in the production plant. Due to technical constraint, it was only possible to use an opening located on the opposite side but at the same height of the sampling unit. Nevertheless, this position is symmetrical compared to the axis of the dryer (see Figure 3).

The position of the probe was the following: the tip of the sapphire window was even with the internal wall of the dryer. The small recess which is formed at this place was cleaned by using the automated nitrogen flushing system. Thereby, the powder accumulated in this recess is blown away after each

(9) Martens, H.; Naes T. *Multivariate Calibration*; Wiley: Chichester, 1996.

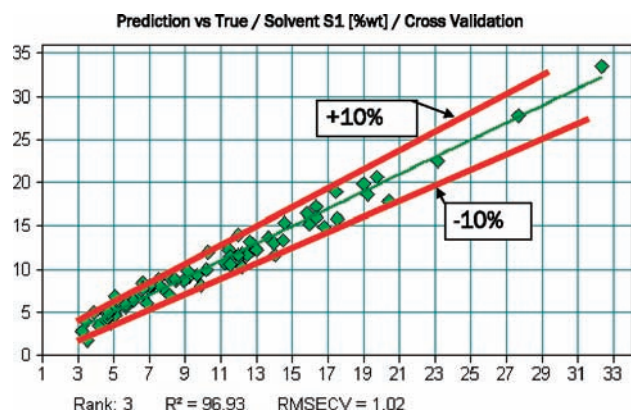


**Figure 5.** Predicted S1 concentrations versus the real concentrations (powder A).

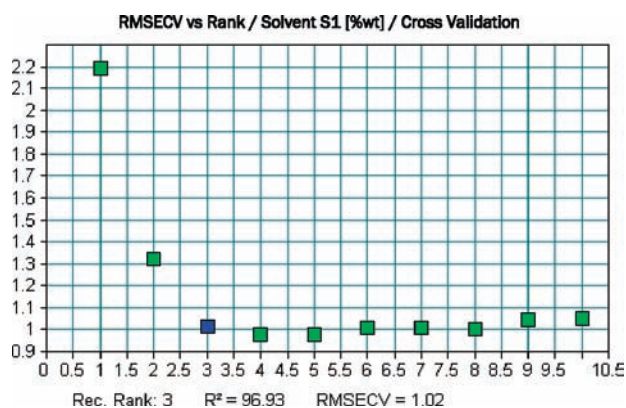


**Figure 6.** RMSECV as a function of the number of factors (solvent S1; powder A).

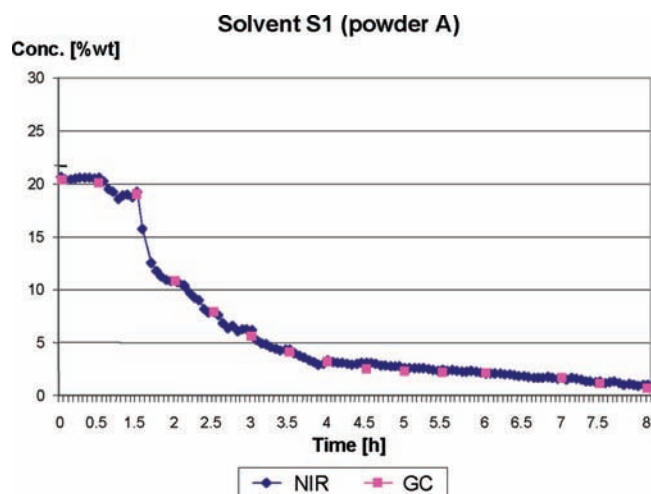


**Figure 7.** Variation of the S1 concentration during the drying process (powder A).

spectral measurement, in such a way that a fresh sample is always on the sapphire window during the data collection.

This installation guarantees that the probe cannot be damaged by the agitator and is always in contact with the powder being measured. Moreover, any contamination of the drug substance with metallic parts of the probe (e.g. due to abrasion) can be avoided with this construction.

The reference analysis of the powder was performed with GC headspace.

Spectra were collected every 10 min during the drying process. After each run, the probe was cleaned by flushing nitrogen with a pressure of 5.5 bar (absolute value) for 5 s. The duration of a spectral determination was 3 min, so that a time of about 7 min was available to accumulate fresh substance in front of the sapphire window. Samples for the GC head space analysis were taken each hour at the beginning of the drying process and every 30 min in the second half of the process.

Collected spectral data and analytical samples from 15 different batches were used to build a chemometric model.

Figure 4 shows some spectra taken during the completion of the drying process. The intensity of the bands decreases during the completion of the process as shown by the arrows on this picture.

Only the shaded parts of the spectra were used for the quantitative evaluation of the data. In these spectra ranges, the influences of the fiber optic cables and of the interferometer of the spectroscope are minimal. The spectra show an important signal noise between 5200 and 5500  $\text{cm}^{-1}$  and between 6800 and 7300  $\text{cm}^{-1}$  (this is due to the presence of water traces in the powder, which in other cases do not necessarily lead to such concern [see the second and third examples]. Water is strongly bound and is not disappearing upon drying because the drying conditions—temperature and vacuum—do not allow the removal of this solvent).

In the case of the solvent S1, the data preprocessing was done with the first derivative and a straight line subtraction. By calculating the first derivative, the signals with steep edges get more emphasis than relatively flat bands. This method is used to emphasize pronounced but small features compared to huge broad-banded structures. Another important application is the evaluation of broad bands. By calculating the first derivative, these structures get a steeper shape which can be evaluated more easily. By using the subtraction of a straight line, a linear tilt of the baseline shift can be eliminated.

For the second solvent S2, the data preprocessing was done with the first derivative and multiplicative scatter correction (MSC). For this purpose, a mean spectrum is calculated from all spectra of the calibration data set. Then, each spectrum  $X(i)$  is transformed according to:

$$X(i)' = u + v \cdot X(i) \quad (2)$$

The coefficients  $u$  and  $v$  are chosen such that the difference between the transformed spectrum  $X(i)'$  and the mean spectrum has a minimum. This method is often used for measurements in diffuse reflection.

The frequency ranges used for the PLS regression, the used data preprocessing, the number of factors, RMSECV (root-mean-square error of cross validation), and  $R^2$  (coefficient of determination) are summarized in Table 1 for S1 and S2. RMSECV was plotted as function of the rank to determine the optimum number of factors (the curve goes through a minimum for the optimal rank). RMSECV is a quantitative measure for the preciseness with which the samples are predicted during a validation.

$$\text{RMSECV} = \sqrt{\frac{1}{M} \cdot \sum_{i=1}^M (Y_i^{\text{meas}} - Y_i^{\text{pred}})^2} \quad (3)$$

$M$  is the number of samples in the calibration set,  $Y_i^{\text{meas}}$  is the true concentration of a sample  $i$ ,  $Y_i^{\text{pred}}$  is the predicted concentration of this sample.

Figure 5 shows the predicted concentrations versus the true concentrations for S1. The range of a relative 10% error is also displayed on this graph. Figure 6 shows the value of RMSECV as a function of the number of factors. This curve is useful for

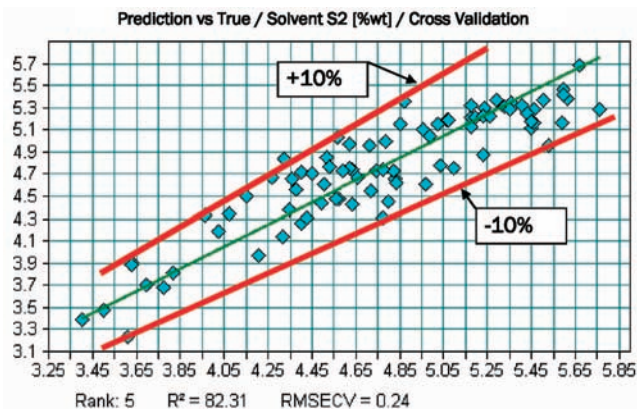


**Figure 8.** Predicted S2 concentrations versus the real concentrations (powder A).

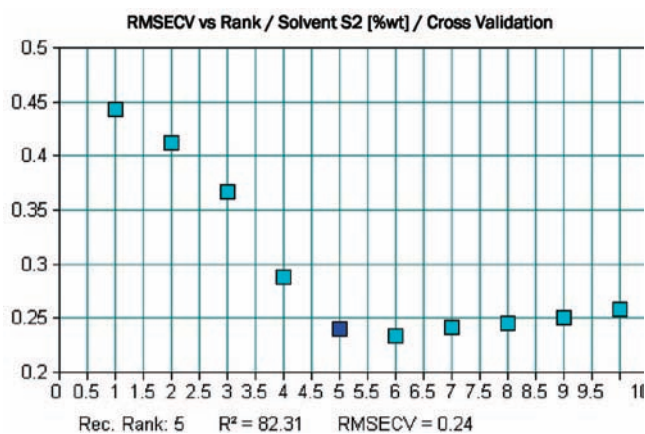


**Figure 9.** RMSECV as a function of the number of factors (solvent S2; powder A).

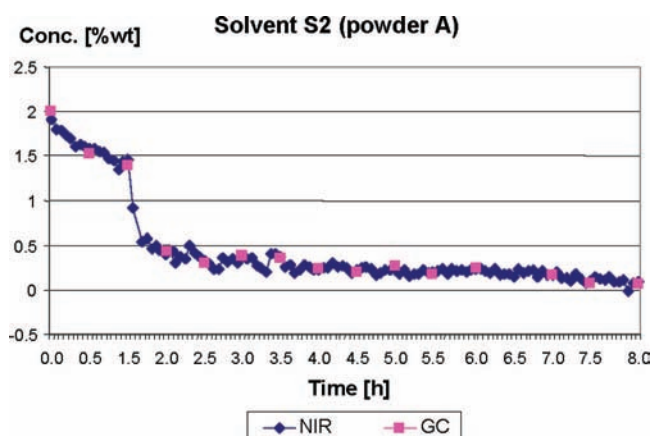


**Figure 10.** Variation of the S2 concentration during the drying process (powder A).

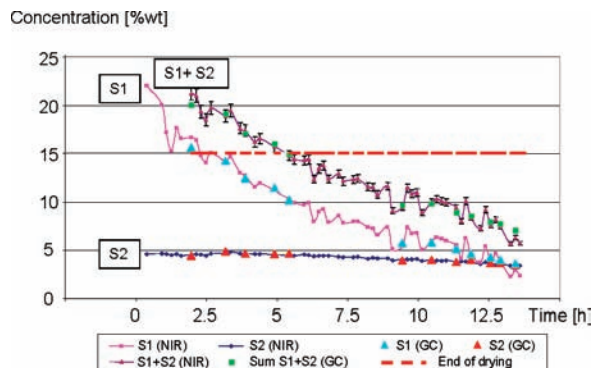


**Figure 11.** Concentrations of solvents S1 and S2 and total solvents' concentration during the drying process (powder A).

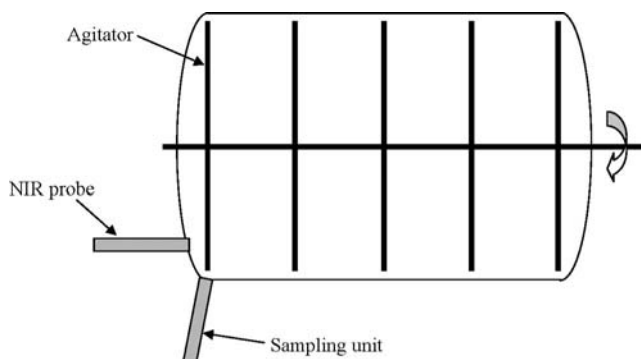


**Figure 12.** Installation of the NIR probe in the paddle dryer (powder B).

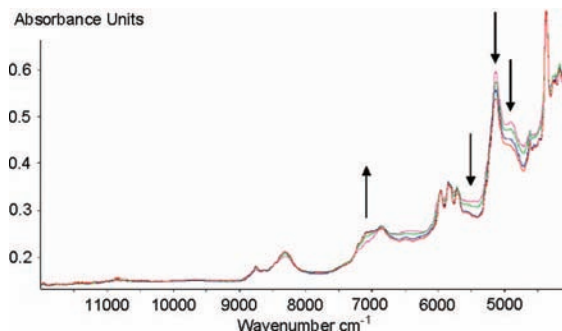


**Figure 13.** Spectra during the drying of powder B in the paddle dryer.

the determination of the optimum number of factors (rank). The values of the RMSECV go through a minimum for the optimal rank (in this case rank 4). In contrast, the value of  $R^2$  possesses a maximum (in this case rank 3). If several ranks lead to comparably good results, it is recommended to select the model with the smallest number of factors.

Figure 7 shows the variation of the S1 concentration during a batch in the manufacturing plant. This graph shows a very good correlation between the results of the NIR measurements and the reference GC analyses.

Figure 8 shows the predicted concentrations versus the real concentrations for the solvent S2. The range of a relative 10% error is also displayed on this graph. Figure 9 shows the value of RMSECV as a function of the number of factors to determine the optimum number of factors.

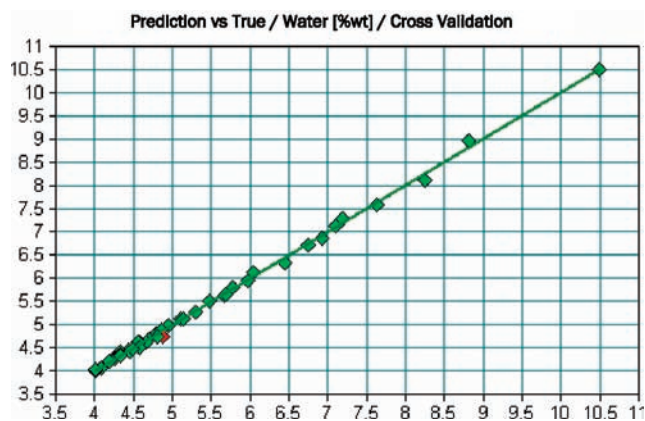
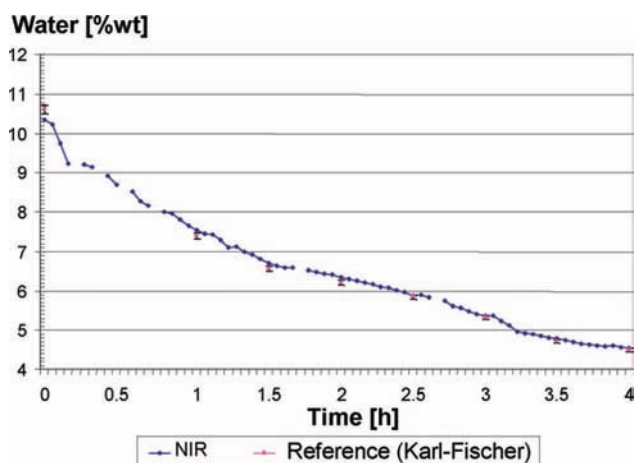
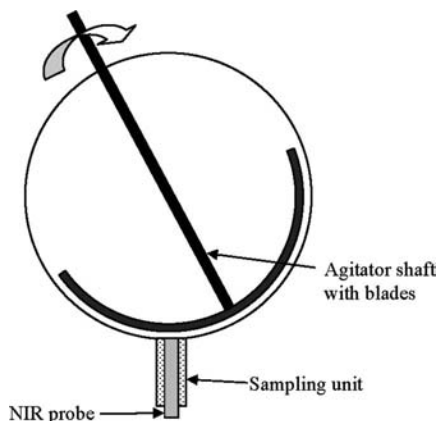
Figure 10 shows the variation of the S2 concentration during a batch in the manufacturing plant. As in the case of S1, the

**Table 2.** Cross validation of the model used for the monitoring of water concentrations (Powder B)

| solvent | frequency range            | data preprocessing                        | number of factors | RMSECV [mass %] | $R^2$ |
|---------|----------------------------|---|-------------------|-----------------|-------|
| water   | 4600–7750 $\text{cm}^{-1}$ | first derivative and vector normalization | 3                 | 0.251           | 99.24 |

results of the NIR measurements are in good agreement with the reference GC analyses.

Figure 11 shows a typical drying process in the production plant. The concentration of both solvents and the sum of these

**Figure 14.** Predicted water concentrations versus the true concentrations (powder B).**Figure 15.** Variation of the water concentration during the drying process (powder B).**Figure 16.** Installation of the NIR probe in the spherical dryer (powder C).

concentrations are represented on this plot. Beside the good agreement between NIR and GC, this figure demonstrates an important possible reduction of the cycle time (in this case about 50%). Moreover, a significant cost reduction is possible due to the reduction of the IPCs (in-process controls).

The obtained chemometric model was validated with the data of the next five batches.

**Second Example: Paddle Dryer.** A paddle dryer consists of a horizontal agitator rotating within a cylindrical housing, which is jacketed for indirect heating. A large number of paddles are attached to the agitator which sweeps close to the inner surface of the housing, moving the material through the dryer. In many cases, heating fluid is circulated through the agitator as well as through the vessel wall. The action of the agitator makes for efficient mixing of the product and good contact with all the heated surfaces (high heat transfer coefficient). Since the agitator is supported at both ends, high-shear or lumpy solids can be handled. On the other hand, the agitator requires seals at both ends, and this aspect of design, operation, and maintenance is critical for the successful operation of the dryer. Discharge of the dried solid is typically via an outlet in the bottom of the cylindrical shell or from the bottom of one of the circular end faces.

The aim of the measurement is to determine the drying end point of the powder B at a residual water content of exactly 4.8 wt % to yield the monohydrate form in a 200 L paddle dryer. Any excessive drying must be avoided to guarantee the product quality. The NIR probe was installed at a low position at the extremity of the dryer, nearly to the sampling unit (see Figure 12).

Data collected during the first drying campaign and samples analyzed by Karl Fischer titration were used to build the chemometric model. Figure 13 shows some spectra taken during the completion of the drying process. The intensity of the bands during the completion of the process decreases or increases as shown by the arrows. The frequency ranges used for the PLS regression, the used data preprocessing, the number of factors, RMSECV and  $R^2$  are summarized in Table 2. Figure 14 shows the predicted concentrations versus the true concentrations for water. This plot demonstrates that an accurate determination of the water concentration with a deviation less than 1% ( $3\sigma$ ) is possible.

Figure 15 shows the variation of the water concentration during a batch in the manufacturing plant. This graph shows a very good correlation between the results of the NIR measurements and the reference titration analyses. This example illustrates the importance of measuring directly in the powder instead of determining the solvent concentration in the vacuum line (or more generally in the vapor phase). The in-line monitoring of this drying process leads to an improvement of the product quality and to a significant reduction of the classical

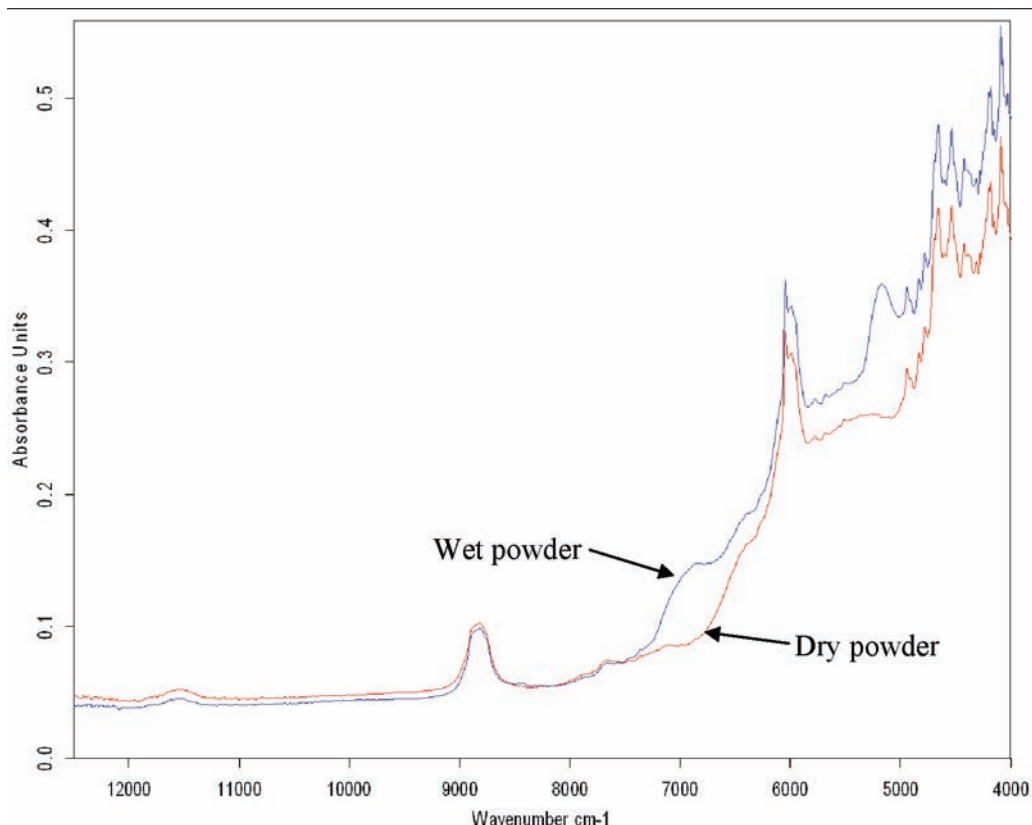


Figure 17. Spectra of wet and dry powder C.

Table 3. Cross validation of the model used for the monitoring of water and S3 concentrations (Powder C)

| solvent | frequency range                             | data preprocessing                         | number of factors | RMSECV [mass %] | $R^2$ |
|---------|---|--|-------------------|-----------------|-------|
| S3      | 5446–6102 $\text{cm}^{-1}$                  | first derivative                           | 3                 | 0.149           | 95.00 |
| water   | 4848–5450 and<br>6098–9300 $\text{cm}^{-1}$ | MSC<br>(multiplicative scatter correction) | 3                 | 0.124           | 99.09 |

in-process controls. Another consequence is a significant reduction of the costs due to the elimination of the out-of-specification batches and to the reduction of the analytical work.

In this case, a determination of the process end point using the monitoring of the water concentration in the vapor phase would be difficult because the process is economically optimized; this means that the substance is dried as fast as possible at relatively high temperatures and under very low pressures.

Therefore, a real concentration plateau can not be observed at a value of 4.8 wt % and an overdrying of the substance is possible, leading to the formation of the anhydride.

**Third Example: Spherical Dryer.** The main goal of the study is the monitoring of an organic solvent S3 and water contents in an active substance (powder C) during the drying process in a spherical dryer. This kind of dryer consists of a machined sphere fitted with either a top- or bottom-mounted

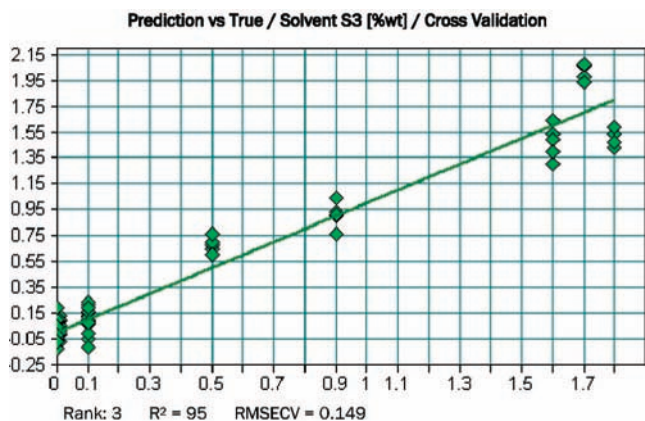


Figure 18. Predicted S3 concentrations versus the real concentrations (powder C).

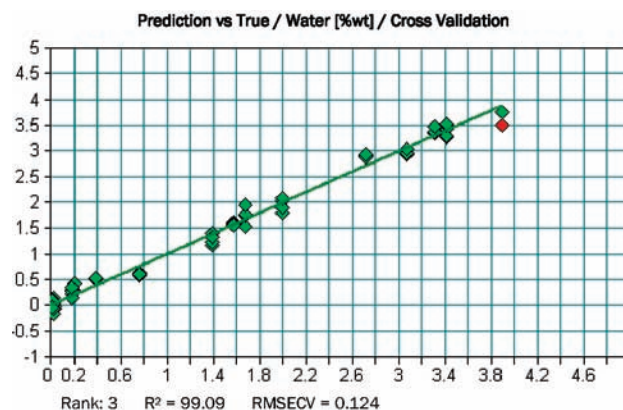
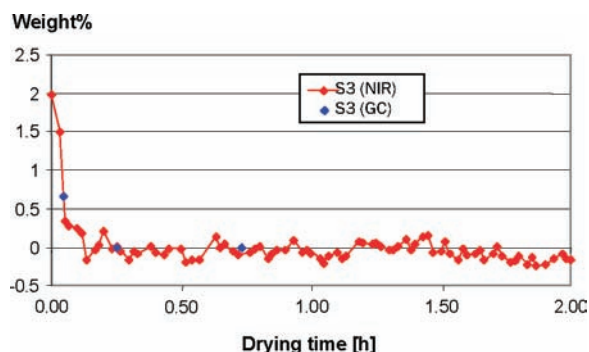
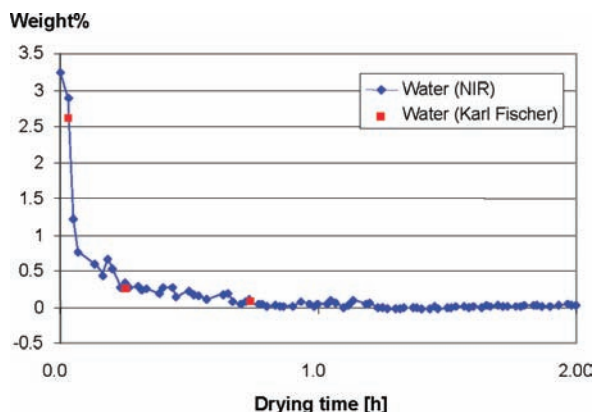


Figure 19. Predicted water concentrations versus the real concentrations (powder C).



**Figure 20.** Variation of the solvent S3 concentration during the drying process (powder C).



**Figure 21.** Variation of the water concentration during the drying process (powder C).

agitator, the latter having a shape specially designed to conform to the spherical wall. The solids outlet is at the very bottom of the sphere, thus allowing almost complete product discharge. The agitator provides excellent solids mixing and contact with the heated wall surface. This results in good heat transfer and drying times, even though the spherical geometry gives this dryer a low ratio of heated wall area to enclosed volume. On the other hand, the spherical shape makes the dryer relatively easy to clean in place, and the cleaning liquid is easily drained out. The geometry also results in a small footprint with respect to installation. In general, the spherical dryer is ideally suited to the drying of pharmaceuticals and other high-value solids.

The NIR probe was installed in the modified sampling unit at the bottom of the dryer (see Figure 16).

Figure 17 shows typical reflectance spectra of the wet and the dry product. The spectrum of the wet product is dominated by the water absorptions, e.g. the typical absorption of water at  $6890\text{ cm}^{-1}$  (first overtone asymmetric OH stretching) or the combination band at  $5175\text{ cm}^{-1}$ .

The parameters used for the PLS regression (frequency ranges, used data preprocessing, the number of factors, RM-SEC, and  $R^2$ ) are summarized in Table 3 for S3 and water.

Figures 18 and 19 show the predicted concentrations versus the real concentrations for the solvent S3 and water. These plots show that an accurate determination of the concentrations with a deviation less than 0.5% ( $3\sigma$ ) is possible. Both models have a low rank of 3 and are in the desired accuracy range for the monitoring of the drying process in the industrial scale.

In this case too, the NIR data and the reference data (headspace GC for the solvent S3, Karl Fischer titration for water) are in very good agreement. Figures 20 and 21 show the variation of the S3 and water concentrations during a batch in the manufacturing plant.

For this example, no significant cycle time reduction is possible because the process duration is relatively short (less than 2 h). Nevertheless, as powder C is a highly active compound, it is very advantageous to perform online monitoring of this drying process to avoid the critical sampling.

## Conclusion

This study demonstrates that NIR is an appropriate method to accurately online monitor drying processes in the industrial scale using different kinds of dryers. The effort necessary to develop the required chemometric model is quickly amortized due to the potentially significant reduction of the drying time and of the traditional analytical work (GC, Karl Fischer, LOD, ...). This reduction of the drying time also leads to an improvement of the plant utilization, which in some cases allows avoiding the expensive installation of additional dryers to reach the desired throughput.

Moreover, this technology allows determining the real residual solvent concentration in the dried substance. The knowledge of this concentration is particularly important if a specific residual humidity must be obtained (e.g., for quality reasons or to get a specific hydrate form).

In the near future, there is no doubt that this kind of equipment will more and more be installed in manufacturing plants to replace the time-consuming classical analyses and decrease the number of out-of-specifications batches.

## Acknowledgment

We are grateful to Dr. M. Wermuth, Dr. H. Geitlinger, and to M. Länzlinger (Solvias AG, Basel) for their active cooperation for the equipment implementation in the production plants, their keen interest in this problem, as well as to Dr. Th. Röder (Novartis Pharma AG) for helpful suggestions and to Dr. R. Schneeberger (Novartis Pharma AG) for supporting this work.

Received for review December 20, 2007.

OP700293P